

## Multimode vibronic model for $\text{Fe}^{2+}$ ions in ZnS

L. Martinelli, M. Passaro, and G. Pastori Parravicini

*Dipartimento di Fisica dell'Università degli Studi di Pisa, Gruppo Nazionale di Struttura della Materia del Consiglio Nazionale delle Ricerche, Centro Interuniversitario di Struttura della Materia del Ministero della Pubblica Istruzione, e Consorzio Interuniversitario Nazionale di Fisica della Materia, piazza Torricelli 2, I-56100 Pisa, Italy*

(Received 10 July 1989)

The vibronic model for  $\text{Fe}^{2+}$  impurities in zinc sulfide crystals is analyzed theoretically with the recursion method. It is shown that the far-infrared absorption spectrum of iron ions can be understood by taking into account the coupling of the electronic state  ${}^5T_2$  to phonons of symmetry  $\Gamma_3$  in three different energy ranges: a low-energy phonon of frequency  $\hbar\omega_1 \approx 25 \text{ cm}^{-1}$ , an intermediate-energy one of frequency  $\hbar\omega_2 \approx 125 \text{ cm}^{-1}$ , and a high-energy one of frequency  $\hbar\omega_3 \approx 300 \text{ cm}^{-1}$ . The corresponding Jahn-Teller energies are estimated as  $E_{JT1} \approx 50 \text{ cm}^{-1}$ ,  $E_{JT2} \approx 130 \text{ cm}^{-1}$ , and  $E_{JT3} \approx 70 \text{ cm}^{-1}$ . Theoretical predictions of the vibronic multimode model for the infrared-absorption spectrum are compared with experimental results and previous speculations available in the literature.

### I. INTRODUCTION

It is commonly accepted that the dynamic Jahn-Teller effect plays an important role<sup>1-3</sup> in the infrared-absorption spectra of transition-metal impurities (for instance,  $\text{Fe}^{2+}$ ) in II-VI compound semiconductors. Although some features and trends in the rich structure of the experimental spectra<sup>4,5</sup> have been interpreted at least qualitatively, a quantitative theoretical analysis of the impurity problem in ZnS is still lacking.

The most formidable obstacle for a theoretical treatment of a vibronic system is the large number of basis functions (or degrees of freedom) required in the product space of the electronic and vibrational states. For example, a  ${}^5T_2$  electronic multiplet linearly coupled with a two-dimensional phonon mode leads to  $15 \times N^2$  degrees of freedom,  $N - 1$  being the number of phonons included. In the case of a multimode vibronic model of the type  ${}^5T_2 \otimes (\Gamma_3 + \Gamma_3)$  the number of basis functions becomes  $15 \times N_1^2 \times N_2^2$ .

Vibronic models for transition-metal impurities in cubic semiconductors have been treated until recently either by means of perturbation theory<sup>1</sup> or by direct diagonalization of matrices of as large a dimension as possible.<sup>2</sup> It is evident that the direct diagonalization, somewhat cumbersome even when one considers only a single mode, becomes intractable in the presence of multimode vibronic systems. On the other hand, from the form of the infrared spectrum of  $\text{Fe}^{2+}$  in ZnS it can be inferred that a single-mode model cannot explain the numerous absorption features.

Very recently, a flexible technique for the theoretical analysis of vibronic systems for transition-metal impurities has been introduced by combining the recursion method with the concepts of dipole-carrying states.<sup>3</sup> Historically we remind the reader that a major breakthrough in the study of systems with a large number of degrees of freedom, described by sparse matrices, has been given by

the Lanczös-Haydock-Heine-Kelly recursion method.<sup>6,7</sup> The method, pioneered by Lanczös,<sup>8</sup> was originally introduced in solid-state physics in connection with electronic problems.<sup>6,7</sup> Then it was extended to coupled electron-boson systems,<sup>9-11</sup> allowing a nonperturbative treatment of the absorption as well as luminescence spectra of typical impurity centers.<sup>12</sup> The formal relationship between the recursion method and the renormalization method has also been established.<sup>13</sup> For what concerns the study of the Jahn-Teller effect in transition-metal impurities, the recursion method was introduced and applied in Ref. 3 to a single-mode vibronic model. The purpose of the present paper is to generalize our procedure and to analyze theoretically a multimode vibronic problem for the infrared spectra of  $\text{Fe}^{2+}$  in ZnS.

An interpretation of the infrared-absorption spectrum of iron impurities in zinc sulfide is a challenging problem indeed; in fact, since the pioneering works of Slack, Ham, and Chrenko<sup>4</sup> it is apparent that a single vibronic mode could not explain such a complex spectrum, which shows a very intense line at  $2945 \text{ cm}^{-1}$ , and two less intense lines at  $2964$  and  $2984 \text{ cm}^{-1}$ , followed by a number of other transitions, empirically interpreted as phonon-assisted transitions. Also, a more recent theoretical interpretation<sup>2</sup> that by necessity could treat only one phonon at a time seems in favor of the conclusion that at least two phonons of different energy must be invoked to explain the absorption spectrum of the impurity centers.

In this paper we solve with the recursion method a number of appropriately chosen single-mode and two-mode vibronic models for  $\text{ZnS:Fe}^{2+}$  and discuss the implications on the far-infrared-absorption spectrum. Some technical aspects on the vibronic model and the calculation procedures are given in Sec. II. The disposable parameters of the vibronic model are determined in such a way to satisfy the very compelling requirements on the energy levels and especially on the relative intensities of the lowest transition lines. This is done in Sec. III, where

the results of the models are discussed and compared with the experiments. Section IV contains the conclusions.

## II. VIBRONIC MODEL AND CALCULATION TECHNIQUE

The infrared-absorption spectrum<sup>4</sup> of  $\text{Fe}^{2+}$  in ZnS, arising from the electronic transitions between the initial  ${}^5E$  and the final  ${}^5T_2$  states of  $\text{Fe}^{2+}$ , shows a sharp peak at  $2945\text{ cm}^{-1}$  followed by a very rich structure extending in energy until about  $3850\text{ cm}^{-1}$ . The very high intensity of the first line with respect to the other ones suggests the supremacy of the spin-orbit interaction over the Jahn-Teller coupling, and consequently a Jahn-Teller energy weaker or of the same order as the spin-orbit-coupling constant. This prediction will be confirmed by the detailed calculations made in Sec. III. However, many phonons of different energies and symmetries can be coupled with the  ${}^5T_2$  excited states, as can be seen from the dispersion curves of ZnS, measured by different authors.<sup>14,15</sup> A useful scheme of the various phonon branches and their symmetry is reported in Ref. 1.

We have already discussed the difficulties of the standard diagonalization procedures to take into account more than one phonon at a time (unless a perturbative approach is justified). This is the essential motivation for using the recursion procedure, which is appropriately implemented here to vibronic systems including two modes of symmetry  $\Gamma_3$  and different energy. Notice, furthermore, that the application of the concepts of parallel computing<sup>16</sup> makes it possible to treat even more complicated vibronic models and will eventually reveal further perspectives in the theoretical interpretation of the wealth of experimental spectra concerning localized impurities in solids. In a cluster model,<sup>17</sup> the mode of symmetry  $\Gamma_5$  is also Jahn-Teller active; however, all the per-

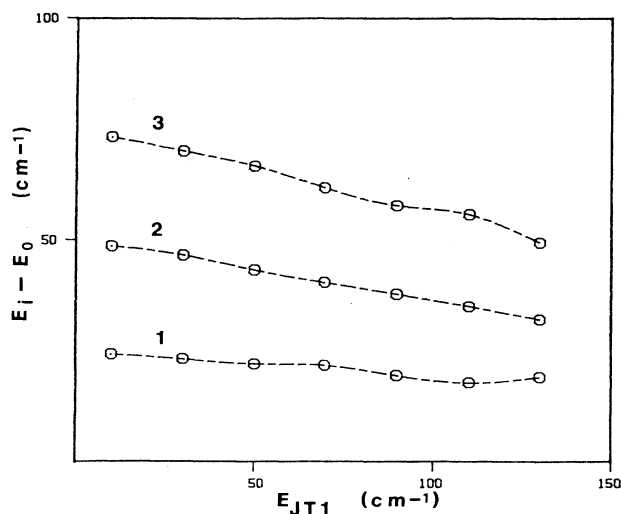


FIG. 1. Energy differences  $E_i - E_0$  ( $i=1,2,3$ ) as a function of the Jahn-Teller energy  $E_{JT1}$ , for a vibronic model with a single phonon,  $\hbar\omega_1 = 25\text{ cm}^{-1}$ .

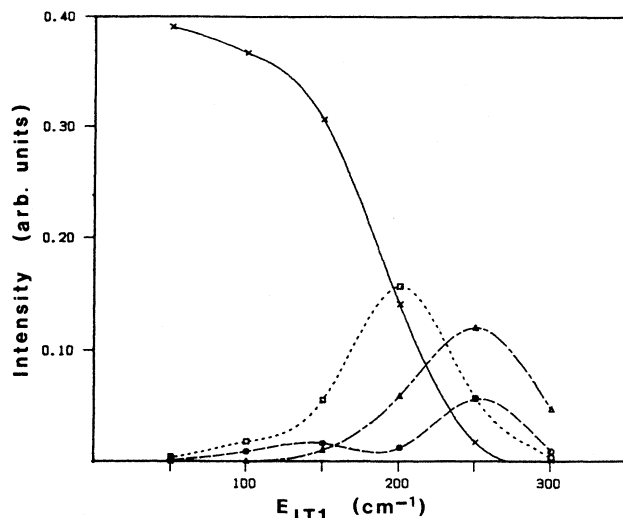


FIG. 2. Intensities  $W(E_i, f_0)$  of the lowest four lines as a function of the Jahn-Teller energy  $E_{JT1}$  for a vibronic model with a single phonon  $\hbar\omega_1 = 25\text{ cm}^{-1}$ .  $\times, \square, \circ, \triangle$  in the order for the first four lines ( $\times$  is for the first line).

vious works,<sup>1,2,18</sup> concerning the Jahn-Teller effect in the infrared-absorption spectrum of this and similar systems, take into account only the coupling with lattice vibrations of  $\Gamma_3$  symmetry. This is justified on the basis of model calculations,<sup>11</sup> which show no drastic difference between the effect of the two different symmetries.

The Hamiltonian of the vibronic system  ${}^5T_2 \otimes (\Gamma_3 + \Gamma_3)$  can be explicitly worked out by appropriately generalizing the treatment of Ref. 3; thus only a few comments are given here. The total Hamiltonian consists of the sum of the electronic contribution including the spin-orbit interaction (throughout the present paper the spin-orbit-coupling constant is that of the free ion,<sup>19</sup> i.e.,  $\lambda = -100\text{ cm}^{-1}$ ), the lattice Hamiltonian, and the linear coupling of the electronic part of two two-dimensional  $\Gamma_3$  phonons, of frequency  $\omega_1$  and  $\omega_2$  and Jahn-Teller energy  $E_{JT1}$  and  $E_{JT2}$ . The basis functions of the vibronic model can be indicated as

$$\Phi_{ij;lm,np} \equiv |\psi_i S_j; lm, np\rangle. \quad (1)$$

Here  $|\psi_i\rangle$  ( $i=1,2,3$ ) are the many electronic wavefunction partners for the irreducible representations  ${}^5T_2$  of the group  $T_d$  (usually labeled  $d_{yz}, d_{xz}, d_{xy}$ );  $|S_j\rangle$  are appropriate combinations of spin functions for  $S=2$  and  $S_z$  from  $+2$  to  $-2$ ;  $(l, m)$  and  $(n, p)$  are the occupation numbers for the partner modes of energy  $\hbar\omega_1$  and  $\hbar\omega_2$ , respectively.

The number of basis functions (1) is the very large quantity  $15 \times N_1^2 \times N_2^2$ , where  $N_1 - 1$  and  $N_2 - 1$  (both numbering  $\approx 10-20$  in the calculations of the present paper) are the number of phonons included in the basis; any direct diagonalization of the Hamiltonian is thus hopeless. The problem is thus handled by transforming with the recursion method the initial and large sparse matrix into a manageable tridiagonal one, whose dimension is

TABLE I. Energy differences  $E_i - E_0$  ( $i = 1, 2$ ) and intensities  $W(E_i, f_0)$  calculated with the recursion method and a single-mode vibronic model of frequency  $\hbar\omega_1 = 25 \text{ cm}^{-1}$ . The reference energy  $E_0$  has been taken equal to zero. Notice that the experimental oscillator strength for  $L_0$ ,  $L_1$ , and  $L_2$  are approximately in the ratio 100:4:1.

$E_{JT1}$ ( $\text{cm}^{-1}$ )	$E_0$ ( $\text{cm}^{-1}$ )	$W(E_0, f_0)$ ( $10^{-3}$ )	$E_1 - E_0$ ( $\text{cm}^{-1}$ )	$W(E_1, f_0)$ ( $10^{-3}$ )	$E_2 - E_0$ ( $\text{cm}^{-1}$ )	$W(E_2, f_0)$ ( $10^{-3}$ )
50	0	391	22	4	43	2
60	0	387	21	6	42	2
70	0	383	21	8	40	3
80	0	379	20	10	39	4
90	0	373	19	13	38	6

the number of iterations performed (in the present case, of the order of 50, with tests up to 100). The hierarchical ordering of states follows the standard iterative procedure. Let  $|f_0\rangle, |f_1\rangle, \dots, |f_\nu\rangle$  denote the first  $\nu+1$  normalized functions of the recursion hierarchy; the  $|F_{\nu+1}\rangle$  (unnormalized) function is evaluated through the three-term recursion relation<sup>6,8</sup>

$$|F_{\nu+1}\rangle = H|f_\nu\rangle - a_\nu|f_\nu\rangle - b_\nu|f_{\nu-1}\rangle. \quad (2)$$

The generic state  $|F_{\nu+1}\rangle$  of the hierarchy can be written as

$$|F_{\nu+1}\rangle = \sum_{\substack{1 \leq i \leq 3, \\ 1 \leq j \leq 5, \\ 0 \leq l, m, n, p \leq \infty}} c_{ij;lm,np}^{(\nu+1)} |\psi_i S_j; lm, np\rangle \quad (3)$$

and the recurrence relation (2) can be transformed into an appropriate recurrence relation of  $c^{(\nu+1)}$ ,  $c^{(\nu)}$ , and  $c^{(\nu-1)}$ . The significant parameters  $b_{\nu+1}^2$  and  $a_{\nu+1}$  are given by the normalization of  $|F_{\nu+1}\rangle$  and by the expectation value of the Hamiltonian; after renormalization of  $|F_{\nu+1}\rangle$ , a new iteration is started.

We choose as the initial state for starting the recursion procedure the dipole-carrying state<sup>3</sup> appropriate for the transition starting from the lower <sup>5</sup>E state. Such a state is the particular linear combination of dipole-allowed states, with coefficients proportional to the matrix elements of the dipole operator. When such a state is chosen as the initial one, all the states generated by the recursion procedure are dipole free. Thus, the Green's function projected on the initial state gives directly the absorption band of the vibronic system.

### III. RESULTS AND COMPARISON WITH THE EXPERIMENTAL DATA

The infrared-absorption spectrum of Fe<sup>2+</sup> in ZnS exhibits a strong line at 2945  $\text{cm}^{-1}$  (referred to herein as  $L_0$ ), followed by two weak lines at 2964 and 2984  $\text{cm}^{-1}$  ( $L_1$  and  $L_2$ ). There are then four rather broad intensity lines at 3051, 3129, 3182, and 3241  $\text{cm}^{-1}$  ( $L_3$ ,  $L_4$ ,  $L_5$ , and  $L_6$ ); after some other structure the absorption spectrum again increases at  $\approx 3500 \text{ cm}^{-1}$  because of the spin-orbit partner band (see Table III and Fig. 5 of Ref. 4). The absorption lines are indicated in the literature with different notations, but for convenience throughout this paper they are indicated with  $L_0, L_1, L_2, \dots$  in increasing energy order.

From the dispersion phonon curves of ZnS, there are several phonon modes (of  $\Gamma_3$  symmetry) of different energy that may become candidates in the vibronic model. On the other hand, even with the powerful recursion method and with expected moderate Jahn-Teller energies, we can treat no more than two phonon modes at one time. Thus we have to decide which modes to embody in the vibronic model and the corresponding coupling parameters.

To settle a reasonably satisfactory criterion for this problem, we begin to observe that the range of energy phonons involved in the experimental absorption data seems to be rather different. The energy differences  $E(L_i) - E(L_0)$  for the lowest lines are, respectively, 19, 39, 106, and 184  $\text{cm}^{-1}$ . These energy differences, taking into account the well-established evidence that  $L_2$  is a replica of  $L_1$ , support the qualitative remark that the boson

TABLE II. Energy differences  $E_i - E_0$  ( $i = 1, 2$ ) and intensities  $W(E_i, f_0)$  calculated with the recursion method and a single-mode vibronic model of frequency  $\hbar\omega_2 = 125 \text{ cm}^{-1}$ . The reference energy  $E_0$  has been taken equal to zero.

$E_{JT2}$ ( $\text{cm}^{-1}$ )	$E_0$ ( $\text{cm}^{-1}$ )	$W(E_0, f_0)$ ( $10^{-3}$ )	$E_1 - E_0$ ( $\text{cm}^{-1}$ )	$W(E_1, f_0)$ ( $10^{-3}$ )	$E_2 - E_0$ ( $\text{cm}^{-1}$ )	$W(E_2, f_0)$ ( $10^{-3}$ )
70	0	386	104	6	201	9
100	0	380	95	7	185	16
130	0	369	86	8	171	25

TABLE III. Energy, intensity  $W(E_i, f_0)$ , and convergence parameter  $W(E_i, f_N)$  calculated with the recursion method and a single-mode vibronic model of frequency  $\hbar\omega_2 = 125 \text{ cm}^{-1}$  and Jahn-Teller energy  $E_{JT2} = 130 \text{ cm}^{-1}$ . The energies are referred to the lowest electronic level,  ${}^5T_2$ . (a) Cluster of 20 phonons and 20 recursions, (b) cluster of 50 phonons and 50 recursions, and (c) cluster of 20 phonons and 50 recursions.

Energy ( $\text{cm}^{-1}$ )	(a) $W(E_i, f_0)$ ( $10^{-3}$ )	$W(E_i, f_N)$	Energy ( $\text{cm}^{-1}$ )	(b) $W(E_i, f_0)$ ( $10^{-3}$ )	$W(E_i, f_N)$	Energy ( $\text{cm}^{-1}$ )	(c) $W(E_i, f_0)$ ( $10^{-3}$ )	$W(E_i, f_N)$
-209.607	369	$0.6 \times 10^{-9}$	-209.607	369	$0.6 \times 10^{-21}$	-209.607	369	$0.3 \times 10^{-21}$
-123.849	8	$0.5 \times 10^{-5}$	-123.858	8	$0.1 \times 10^{-14}$	-123.858	8	$0.8 \times 10^{-15}$
-38.075	28	$0.6 \times 10^{-4}$	-38.882	25	$0.2 \times 10^{-9}$	-38.882	25	$0.2 \times 10^{-9}$
			-29.298	3	$0.6 \times 10^{-8}$	-29.298	3	$0.5 \times 10^{-8}$
56.626	8	$0.6 \times 10^{-2}$	53.117	5	$0.6 \times 10^{-5}$	53.117	5	$0.7 \times 10^{-5}$
			70.779	0.4	$0.7 \times 10^{-3}$	69.574	0.4	$0.7 \times 10^{-3}$
			90.011	5	$0.6 \times 10^{-4}$	89.910	5	$0.5 \times 10^{-4}$
133.700	13	$0.2 \times 10^{-1}$	148.289	9	$0.3 \times 10^{-4}$	148.230	9	$0.3 \times 10^{-4}$
226.259	30	$0.2 \times 10^{-1}$	202.259	16	$0.6 \times 10^{-4}$	200.332	16	$0.8 \times 10^{-4}$
			278.445	31	$0.1 \times 10^{-2}$	274.656	21	$0.3 \times 10^{-2}$
313.536	401	$0.2 \times 10^{-2}$	307.129	230	$0.1 \times 10^{-2}$	304.043	199	$0.2 \times 10^{-2}$
			326.213	157	$0.1 \times 10^{-2}$	324.194	198	$0.1 \times 10^{-2}$

frequencies of interest are reasonably different. When this is the case (and provided that the electronic state is nondegenerate), the boson modes are expected to relax independently<sup>20</sup> and the correlation function in the time domain is the product of the correlation functions of the contributing modes; however, in our specific problem interference effects may become important. Thus we begin to consider the energy and the intensity of the first lowest lines supposing only one phonon-active mode; later we refine the vibronic model by considering interference effects, automatically included in a multimode vibronic model.

A vibronic model with one phonon mode has two adjustable parameters, i.e.,  $\hbar\omega_1$  and  $E_{JT1}$ ; the relative energy position of the lowest lines  $L_0, L_1, L_2$  and the relative order of magnitude of their intensity pose quite restrictive constraints and allow us to fix with satisfactory accuracy  $\hbar\omega_1$  and  $E_{JT1}$ . The low-frequency phonon  $\hbar\omega_1 = 25 \text{ cm}^{-1}$  is found to be in the region of TA branches inside the Brillouin zone, in agreement with previous authors. In Fig. 1 we show the behavior of the energy differences  $E_i - E_0$ ,  $i = 1, 2, 3$ , versus the Jahn-Teller energy  $E_{JT1}$ , with the choice of  $\hbar\omega_1 = 25 \text{ cm}^{-1}$ . The crystal-field parameter  $|Dq|$  has been chosen, here and throughout the whole paper, in such a way to fix the first spectral line at  $2945 \text{ cm}^{-1}$ . The parameter  $|Dq|$  (of the order of about  $300 \text{ cm}^{-1}$ ), although slightly dependent on  $E_{JT}$ , is the less relevant aspect of the model, since its effect is merely to shift rigidly all the transition energies; it does not influence the energy differences and intensities of the lines.

Figure 2 is the counterpart of Fig. 1 for what concerns the behavior of the intensities  $W(E_i, f_0)$  versus  $E_{JT}$  of the first four lines of the model. The quantity  $W(E_i, f_0)$  is given by the modulus square of  $\langle \Psi_i | f_0 \rangle$ , where  $|\Psi_i\rangle$  is the eigenfunction of the vibronic model, and is obtained by diagonalization of the chain recursion Hamiltonian (after convergence is reached). We recall that, choosing

as an initial state  $|f_0\rangle$  of the recursion the dipole-carrying state, the projected density of states  $|\langle \Psi_i | f_0 \rangle|^2$  is proportional to the absorption spectrum. The most remarkable feature of Fig. 2 is the significant quenching of the intensity of the first line when  $E_{JT1}$  increases. A similar behavior is also found for all the other phonon frequencies we have examined. Since the experiments give evidence of a very strong first line with respect to the rest of the spectrum, the region of possible Jahn-Teller coupling is strongly restrained. From Figs. 1 and 2 we deduce that acceptable values for  $E_{JT1}$  are in the range  $50\text{--}100 \text{ cm}^{-1}$  (more accurate results on the intensities could further limit this range). In Table I we report  $E_i - E_0$  ( $i = 1, 2$ ) and  $W(E_i, f_0)$  calculated with  $\hbar\omega_1 = 25 \text{ cm}^{-1}$  for some values of  $E_{JT1}$ , and we see that a satisfactory understanding of the experimental lines  $L_0, L_1, L_2$ , both for what concerns their relative energy and their relative intensity, is achieved.

From the above calculations it is evident that the interpretation of higher lines in the spectrum, and in particular  $L_3$  and  $L_4$ , requires phonons of completely different energy. We begin to neglect interference effects and select a phonon of intermediate frequency  $\hbar\omega_1 = 125 \text{ cm}^{-1}$ , corresponding to a TA(K) phonon of ZnS. As before, we examine both the behavior of  $E_i - E_0$  and that of  $W(E_i, f_0)$  at different values of  $E_{JT2}$ . In this way we can individuate a good zone for the parameter  $E_{JT2}$ , in the range  $70\text{--}130 \text{ cm}^{-1}$ . In Table II we report some of the results obtained for  $E_i - E_0$  and  $W(E_i, f_0)$  at different values of  $E_{JT2}$ .

Our desire is now to refine the vibronic model by studying simultaneously the effect of two two-dimensional phonons; but before doing this we have to discuss some numerical aspects of the simpler one-phonon-active vibronic model in order to find a computationally workable procedure.

To check the accuracy of the single-mode model we have varied the dimension of the phonon cluster and the

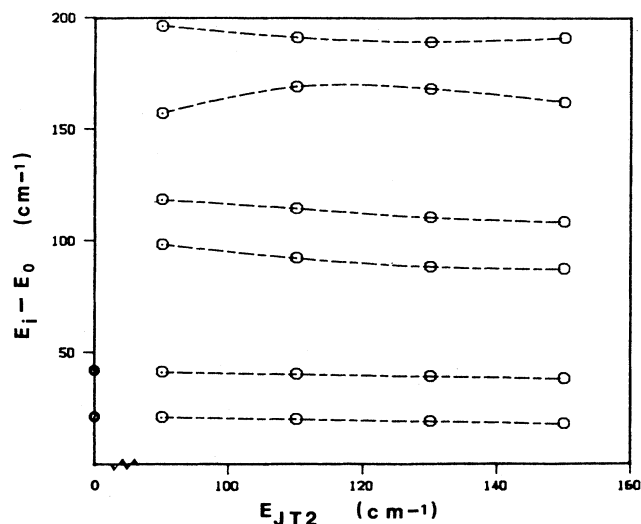


FIG. 3. Energy differences  $E_i - E_0$  as a function of the Jahn-Teller energy  $E_{JT2}$  for a vibronic model with two phonons. The parameters are  $\hbar\omega_1 = 25 \text{ cm}^{-1}$ ,  $E_{JT1} = 50 \text{ cm}^{-1}$ , and  $\hbar\omega_2 = 125 \text{ cm}^{-1}$ .

number of the recursions made, allowing also for some overrecursions. The convergence of the eigenvalues has been tested by calculating the quantity  $W(E_i, f_N)$ , defined as the projection modulus square  $|\langle \Psi_i | f_N \rangle|^2$  of the chain eigenfunction  $\Psi_i$  on the last available chain state  $f_N$ . The quantities  $W(E_i, f_N)$  give an indication of the localization and accuracy of the eigenvalue  $E_i$  after  $N$  recursions. Notice that in the literature<sup>10,21</sup> the “accuracy parameter” is often provided via the alternative quantity  $\rho(E_i, f_N)$ , called the “residual vector” and defined as  $\rho(E_i, f_N) = |\langle \Psi_i | f_N \rangle b_{N+1}|$ . In Table III we summarize the results obtained, for instance, for  $\hbar\omega_2 = 125 \text{ cm}^{-1}$  and  $E_{JT2} = 130 \text{ cm}^{-1}$ , using (a) a cluster of 20 phonon and 20 recursions, (b) a cluster of 50 phonons and 50 recursions, and (c) a cluster of 20 phonons and 50 recursions. For

convenience of comparison the theoretical energies reported in Table III do not include the crystal-field-effect shift. An analysis of Table III (and other similar tables) shows that 20 recursions are not enough for calculating more than three eigenvalues or so; instead, a cluster of 20 phonons and 50 recursions gives results very similar (at the lower energies practically identical) to those with no overrecursions, at least in the  $400\text{-cm}^{-1}$  energy range following the first eigenvalue. In considering a multimode vibronic model, we consider still manageable clusters of 20 phonons (for each type and partner) and perform 50 recursions.

In order to clarify the role of interference effects in the  ${}^5T_2 \otimes (\Gamma_3 + \Gamma_3)$  model, we begin by choosing the frequencies  $\hbar\omega_1 = 25 \text{ cm}^{-1}$  and  $\hbar\omega_2 = 125 \text{ cm}^{-1}$ . Taking a fixed value for  $E_{JT1}$  ( $E_{JT1} = 50 \text{ cm}^{-1}$ ) we have varied  $E_{JT2}$ . The results obtained are summarized in Fig. 3. We have reported, for  $E_{JT2} = 0$ , only the first two values of the energy differences  $E_i - E_0$ , because the intensity of the following lines are negligible with respect to the previous ones. For  $E_{JT2} \neq 0$  we see two low-intensity lines coming from the phonon  $\hbar\omega_1$ , slightly influenced by the phonon  $\hbar\omega_2$ , and corresponding to the experimental  $L_1, L_2$  lines. Then we find two other lines of low intensity, separated by about  $20 \text{ cm}^{-1}$ , coming from the phonon  $\hbar\omega_2$  and its interference with the phonon  $\hbar\omega_1$ . It seems reasonable to attribute these two lines at about  $100 \text{ cm}^{-1}$  to the experimental peak  $L_3$  at  $106 \text{ cm}^{-1}$  from the first transition. At about  $180 \text{ cm}^{-1}$  from  $E_0$  we find two other transitions, somewhat more intense than the previous ones and separated by about  $20 \text{ cm}^{-1}$ . Also, this doublet is due to the interference effects of the two phonons considered, and corresponds to the experimental transition at  $184 \text{ cm}^{-1}$  from  $L_0$ .

In the Table IV we show, for  $E_{JT2} = 130 \text{ cm}^{-1}$  and  $|Dq| = 313.6 \text{ cm}^{-1}$ , the experimental energy transitions calculated, the intensities calculated, and the convergence parameter. A reasonable interpretation of the transitions up to about  $200 \text{ cm}^{-1}$  from  $L_0$  is achieved, but for still higher energy transitions it is apparently necessary that we consider a vibronic model which includes a higher-

TABLE IV. Energy, intensity  $W(E_i, f_0)$ , and convergence parameter  $W(E_i, f_N)$  calculated with the recursion method and two-phonon vibronic model. The parameters are  $\hbar\omega_1 = 25 \text{ cm}^{-1}$ ,  $E_{JT1} = 50 \text{ cm}^{-1}$ ,  $\hbar\omega_2 = 125 \text{ cm}^{-1}$ ,  $E_{JT2} = 130 \text{ cm}^{-1}$ , and  $|Dq| = 313.6 \text{ cm}^{-1}$ . Experimental data are also reported for comparison.

Transition energy ( $\text{cm}^{-1}$ )		$W(E_i, f_0)$ ( $10^{-3}$ )	$W(E_i, f_N)$
Calc.	Expt. <sup>a</sup>		
2945.0	2945	336	$0.1 \times 10^{-9}$
2964.2	2964	12	$0.3 \times 10^{-6}$
2983.7	2984	8	$0.9 \times 10^{-5}$
3009.4		1	$0.1 \times 10^{-2}$
3033.2		9	$0.6 \times 10^{-3}$
3054.5	3051	12	$0.5 \times 10^{-3}$
3112.7		12	$0.2 \times 10^{-2}$
3133.8	3129	10	$0.3 \times 10^{-3}$

<sup>a</sup>Reference 4.

energy frequency. We have thus considered a vibronic model which contains an intermediate-frequency phonon ( $\hbar\omega_2=125\text{ cm}^{-1}$ ) with one at higher energy ( $\hbar\omega_3=295\text{ cm}^{-1}$ ) corresponding to a TO(L) phonon of ZnS. Although this model neglects interference effects with  $\hbar\omega_1$ , it is expected to be, nevertheless, of value. However, because of the absence of the weak energy phonon, we do not expect to reproduce well the low-energy part of the spectrum. At higher energy, calculations show that a medium-intensity line occurs near  $240\text{--}250\text{ cm}^{-1}$ , far from the first one. The prevalence of the  $L_0$  line again limits the energy range of acceptable values of  $E_{JT3}$  to  $50\text{--}80\text{ cm}^{-1}$ . Thus the whole spectrum can be interpreted in a satisfactory way with a linear Jahn-Teller interaction comprehensive of the contribution of more than one phonon (a low-, an intermediate-, and a high-energy one) of symmetry  $\Gamma_3$ , coupled with the motion of the electrons with a Jahn-Teller energy lower (or the same order) than the spin-orbit-coupling parameter.

#### IV. CONCLUSIONS

In this paper we have analyzed theoretically a multimode vibronic model of the complex infrared-absorption spectrum of iron impurities in ZnS; we have found that low-, intermediate-, and high-energy phonons are to be taken into account and we have estimated the corresponding Jahn-Teller energy. The importance of this study goes beyond the vibronic models examined here, but it shows a flexible procedure whose systematic use should allow a more satisfactory understanding of vibronic systems where interference effects between phonons of different energy are not negligible. Furthermore, interesting perspectives are likely to be revealed by the application of the concepts of parallel computing, which should allow one to solve more complicated vibronic systems, and add to the present body of literature consisting of accurate experimental data and interpretations of a qualitative nature.

- 
- <sup>1</sup>F. S. Ham and G. A. Slack, *Phys. Rev. B* **4**, 777 (1971).  
<sup>2</sup>J. Rivera-Iratchet, M. A. De Orúe, and E. E. Vogel, *Phys. Rev. B* **34**, 3992 (1986); E. E. Vogel, J. Rivera-Iratchet, and M. A. de Orúe, *ibid.* **38**, 3556 (1988).  
<sup>3</sup>L. Martinelli, M. Passaro, and G. Pastori Parravicini, *Phys. Rev. B* **39**, 13 343 (1989).  
<sup>4</sup>G. A. Slack, F. S. Ham, and R. M. Chrenko, *Phys. Rev.* **152**, 376 (1966).  
<sup>5</sup>J. M. Baranowski, J. W. Allen, and G. L. Pearson, *Phys. Rev.* **160**, 627 (1967); see also M. Jezewski, Z. Liro, and J. M. Baranowski, *J. Phys. C* **20**, 311 (1987).  
<sup>6</sup>R. Haydock, V. Heine, and M. J. Kelly, *J. Phys. C* **5**, 2845 (1972); **8**, 2591 (1975). Also see the volume by D. W. Bullt, R. Haydock, V. Heine, and M. J. Kelly, in *Solid State Physics*, edited by H. Erhenreich, F. Seitz, and D. Turnbull (Academic, New York, 1980), Vol. 35.  
<sup>7</sup>G. Grosso and G. Pastori Parravicini, *Adv. Chem. Phys.* **62**, 81 (1985); **62**, 133 (1985), and references quoted therein.  
<sup>8</sup>C. Lanczós, *J. Res. Nat. Bur. Stand. (U.S.)* **45**, 255 (1950); **49**, 33 (1952); *Applied Analysis* (Prentice-Hall, Englewood Cliffs, NJ, 1956).  
<sup>9</sup>S. Muramatsu and N. Sakamoto, *J. Phys. Soc. Jpn.* **44**, 1640 (1978); **46**, 1273 (1979); *Phys. Rev. B* **17**, 868 (1978).  
<sup>10</sup>M. C. M. O'Brien and S. N. Evangelou, *J. Phys. C* **13**, 611 (1980); *Solid State Commun.* **36**, 29 (1980); M. C. M. O'Brien, *J. Phys. C* **16**, 85 (1983); **16**, 6345 (1983); **18**, 4963 (1985).  
<sup>11</sup>L. Martinelli and G. Pastori Parravicini, *Phys. Rev. B* **37**, 10 612 (1988).  
<sup>12</sup>L. Martinelli, G. Pastori Parravicini, and P. L. Soriani, *Phys. Rev. B* **32**, 4106 (1985).  
<sup>13</sup>P. Giannozzi, G. Grosso, S. Moroni, and G. Pastori Parravicini, *Appl. Num. Math.* **4**, 273 (1988); G. Grosso, S. Moroni, and G. Pastori Parravicini, *Phys. Scr.* **T25**, 316 (1989).  
<sup>14</sup>J. Bergsma, *Phys. Lett. A* **32**, 324 (1970).  
<sup>15</sup>N. Vagelatos, D. Wehe, and J. S. King, *J. Chem. Phys.* **60**, 3613 (1974).  
<sup>16</sup>See, for instance, K. C. Bowler, A. D. Bruce, R. D. Kenway, G. S. Pawley, and D. J. Wallace, in *Proceedings of the 7th General Conference of the Condensed Matter Division of the European Physical Society*, edited by F. Bassani, G. Grosso, G. Pastori Parravicini, and M. P. Tosi [*Phys. Scr.* **T19A**, 32 (1987)].  
<sup>17</sup>M. D. Sturge, in *Solid State Physics*, edited by F. Seitz, D. Turnbull, and H. Ehrenreich (Academic, New York, 1967), Vol. 20.  
<sup>18</sup>H. Maier and U. Scherz, *Phys. Status Solidi B* **62**, 153 (1974).  
<sup>19</sup>C. E. Moore, *Atomic Energy Levels*, Nat. Bur. Stand. (U.S.) Circ. No. 467 (U.S. GPO, Washington, D.C., 1949), Vol. II (1952).  
<sup>20</sup>A. Testa, W. Czaja, A. Quattropani, and P. Schwendimann, *J. Phys. C* **20**, 1253 (1987).  
<sup>21</sup>D. R. Pooler in *The Dynamical Jahn-Teller Effect in Localized Systems*, Vol. 7 of *Modern Problems in Condensed Matter*, edited by Yu. E. Perlin and M. Wagner (North-Holland, Amsterdam, 1984).